Submitted for Review *Journal of Offshore Mechanics and Arctic Engineering,* ASME

Practical Airgap Prediction for Offshore Structures

Bert Sweetman, PhD
Assistant Professor
Maritime Systems Engineering Department
Texas A&M University at Galveston
200 Seawolf Parkway
Galveston, Texas 77553, USA
sweetman@tamu.edu

Abstract

Two new methods are proposed to predict airgap demand. Airgap demand is is the maximum expected increase in the water surface elevation caused incident waves interacting with an offshore structure. The first new method enables inclusion of some second-order effects, though it is based on only first-order diffraction results. The method is simple enough to be practical for use as a hand-calculation in the early stages of design. Two existing methods of predicting airgap demand based on first-order diffraction are also briefly presented and results from the three methods are compared with model test results. All three methods yield results superior to those based on conventional post-processing of first-order diffraction results, and comparable to optimal post-processing of second-order diffraction results. A second new method is also presented; it combines extreme value theory with statistical regression to predict extreme airgap events using model test data. Estimates of extreme airgap events based on this method are found to be more reliable than estimates based on extreme observations from a single model test. This second new method is suitable for use in the final stages of design.

Introduction and Background

Present airgap design methodologies for floating structures are not standard and rely heavily on empirical knowledge and model tests. Large production semi-submersibles and novel large-volume offshore structures provide design challenges that are well outside the present design experience base. Unlike drilling semisubmersibles, these vessels are generally required to remain on station throughout the most severe weather. Urgency is added by the fact that airgap design problems (wave impacts) have been encountered on large North Sea semi-submersibles, including the Veslefrikk B platform in the Norwegian sector of the North Sea, the vessel which is the subject of the analysis and model tests presented in this paper.

High volume structures, whether fixed or floating, complicate the airgap calculation by significantly diffracting the incident waves. For these structures, ignoring diffraction effects is non-conservative in that diffraction effects generally worsen the airgap demand. Large-volume floating structures, including semisubmersibles and floating production, storage and offloading vessels (FPSO's), offer the most significant challenge. Two distinct hydrodynamic effects are observed: (1) global forces and resulting motions are significantly affected by diffraction; and (2) the local wave elevation, $\eta(t)$, is also significantly influenced by diffraction. For semisubmersibles, these wave amplification effects are most extreme at locations above a pontoon and/or near a major column.

Here, four methods for prediction of airgap demand without use of second-order diffraction are presented and compared with model test results. First, a theoretical overview and motivation section outlines which physical terms are included in conventional first- and second-order diffraction analysis and the implications of the assumptions implicit to various post-processing methods. Some background is then presented which is relevant to all of the methods presented here. This background includes airgap notation, model testing issues and methodologies and some statistical background. Two existing and one new method of predicting airgap demand using results from only first-order diffraction are then presented and critically compared with model test data. It is concluded that second-order effects should be included in airgap prediction throughout the early stages of design, but that these methods are inadequate for final design. Another new methodology is then presented which is useful for final design. In the new methodology extreme value theory and regression techniques are combined to predict extremes from model test results.

Theoretical Overview and Motivation

The disturbed water surface in the presence of the vessel, $\eta(t)$, is assumed to be a sum of incident and diffracted waves, η_i and η_d, each of which is a sum of first- and second-order components:

$$\eta(t) = \eta_i(t) + \eta_d(t) \quad (1)$$

$$\eta_i(t) = \eta_{1,i}(t) + \eta_{2,i}(t) \quad (2)$$

$$\eta_d(t) \quad = \quad \eta_{1,d}(t) + \eta_{2,d}(t) \tag{3}$$

This assumption is consistent with most state-of-the-art nonlinear hydrodynamic analyses, which employ second-order perturbation solutions. Combining Eqs. 1–3:

$$\eta(t) = \eta_{1,i}(t) + \eta_{1,d}(t) + \eta_{2,i}(t) + \eta_{2,d}(t) \tag{4}$$

In a conventional second-order analysis, all four terms in the sum are considered. In a first-order analysis, only the first two terms are considered, i.e., second-order effects in both the incident wave and diffraction processes are neglected. In the "hybrid" methods investigated here, second-order effects of the incident waves are considered, while second-order diffraction effects are neglected. Thus, the methods proposed here lie between first- and second-order analysis.

Three methods of applying first-order diffraction results to predict airgap demand including some second-order effects are compared in this paper. The difference between the two existing methods is in the application of the Stokes second-order wave component. In the method denoted "Stokes second-order," a square matrix of Stokes second-order transfer function components is developed and applied as in Eqs. 18–21 (to be discussed). In the method based on narrow-band theory, the extreme of the total wave process, $\eta(t)$, is assumed to coincide in time with that of $\eta_1(t)$; it is therefore only necessary to model second-order effects during that single, largest wave cycle, so the Stokes second-order contribution is calculated for only that largest wave. Special consideration of only the single largest wave cycle is conceptually similar to the design wave approach. The new method proposed here, "First-Order with Statistical Correction," implicitly assumes that the airgap demand resulting from the incident wave is statistically similar to the incident wave and applies a statistical correction to approximate the non-linear effects.

The advantage of any of these "hybrid" approaches is computational simplicity: $\eta_{1,d}$ requires only (relatively straightforward) linear diffraction analysis, and $\eta_{2,i}$, is available analytically from second-order Stokes theory. The latter two methods are of sufficient computational simplicity to allow inclusion of second-order effects as a hand-calculation, while the first of the three methods requires solution of an eigenvalue problem.

Second-order diffraction analyses are available (e.g. [3]) but these second-order methods are difficult to apply and presently lack widespread use and verification in modeling the nonlinear diffracted wave surface. Standard airgap response prediction uses linear theory, which generally does not effectively reproduce measurements from model tests [2, 4–6]. First-order diffraction is often selected over the more powerful second-order because of its relative simplicity, ease of use and robustness of the solution. While second-order diffraction effects are expected to better reflect observed data, these radiation/diffraction panel calculations have been found sometimes to over-predict airgap demand [4, 7].

Neglecting second-order diffraction substantially simplifies computations but is clearly expected to underestimate the spatial variability in diffraction effects; such an underestimation has previously been shown for this platform [2]. The results presented later in Figure 5, however, show that optimal use of second-order

diffraction results also underestimates this spatial variability. A goal here is to understand the numerical impact of this simplification through use of three different stochastic models.

Airgap Notation and Modeling Issues

Figure 1 shows a schematic view of a semi-submersible platform, both before and after waves are applied. In the absence of waves, the still-water airgap distance is denoted a_0. In the presence of waves, $\eta(t)$ denotes the wave surface elevation relative to a vertically fixed observer at a particular horizontal location along the moving structure. The corresponding vertical motion of the platform is denoted $\delta(t)$. If $\eta = \delta$, the airgap would remain equal to its still-water value, a_0. More generally, the airgap response $a(t)$ will be reduced from a_0 by the difference, $\eta(t) - \delta(t)$:

$$a(t) = a_0 - [\eta(t) - \delta(t)] \tag{5}$$

Deck impact occurs if the airgap $a(t) < 0$. Among the various terms in Eq. 5, the vertical offset $\delta(t)$ is perhaps the most straightforward to model. Linear diffraction results may often suffice to accurately model this offset. In contrast, the free surface elevation, $\eta(t)$, generally shows nonlinear behavior—and hence represents a non-Gaussian process. Modeling attention is therefore focused here on $\eta(t)$. This separation of vessel motions from diffraction effects on the water surface is fairly standard in hydrodynamic post-processing, and is consistent with typical hydrodynamic diffraction analysis. This separation also makes these methods applicable to fixed offshore structures.

Description of Model Test Data

Test data used here for verification of the theoretical models come from a 1:45 length-scale model of Veslefrikk, which was tested in the wave tank at Marintek using various types of irregular waves [8]. Figure 2 shows a plan view of the platform, together with the 9 locations for which the airgap responses have been measured as a function of time. Note that airgap probes with lower numbers are generally further up-stream, i.e., closer to the wave generator. All tests studied here apply long-crested waves traveling along the diagonal of the structure.

The platform rigid-body motions in heave, roll, and pitch—denoted ξ_3, ξ_4, and ξ_5—have also been recorded. Sign conventions must be consistent with the model test data; here, ξ_3 is positive in the upward direction, ξ_4 is positive rolling to port, and ξ_5 is positive pitching bow-down. The measured motions permit estimation of the net vertical displacement, $\delta(t)$, at any location (x, y) of interest:

$$\delta(t) = \xi_3(t) + y \cdot \sin(\xi_4(t)) - x \cdot \sin(\xi_5(t)) \tag{6}$$

The time-history of the elevation of the water-surface relative to a fixed observer is inferred using Eq. 5 and

the measured airgap, $a(t)$, and the estimate of $\delta(t)$ as:

$$\eta(t) = a_0 - a(t) + \delta(t) \tag{7}$$

Table 1 summarizes the geometric properties of the platform as configured for the tests used here. Prior to the model test, waves are first generated in the model test basin in absence of the model. The incident wave, $\eta_i(t)$, is measured at location 7 (Figure 2), where the platform is to be centered.

Following common practice, wave histories have been generated from a stationary random process model, applied over a fixed "seastate" duration of T_{ss}=3 hours. Its spectral density function, $S_\eta(f)$, is described by the significant wave height H_s=$4\sigma_\eta$, the peak spectral period, T_P, and the spectral peakedness factor γ associated with the JONSWAP spectrum (e.g. [9] from [10]). Table 2 describes the H_s, T_P, and γ values for each of the three test conditions. The peakedness factor, γ, is the ratio of the maximum spectral density to that of the corresponding Pierson-Moskowitz spectrum (e.g. [9]). The γ reported for the bimodal spectrum is an approximation of the peakedness parameter for an equivalent JONSWAP spectrum. An actual JONSWAP spectrum with the parameters indicated for this bimodal spectrum would not be realizable due to wave breaking.

Statistical Background: Prediction of Extremes

Three of the four methods presented in this paper predict extreme values by first predicting the desired fractile of a Gaussian process (e.g., fractiles of the maximum response over a fixed duration) and then relying on the Hermite model to transform that fractile of the standard normal distribution to the equivalent fractile of a non-Gaussian response.

Gaussian Extremes

Extreme values of a random variable which is assumed to follow a standard-normal, or Gaussian, distribution can be predicted by assuming upcrossings of high levels of $u(t)$ follow a Poisson process (e.g. [11] from [12, 13]) so that:

$$P[U_{max} \leq u] = e^{-\nu_0 T e^{-u^2/2}} \tag{8}$$

where ν_0 is the average up-crossing rate and T is the duration. The number of cycles, N, is given by $N = \nu_0 \times T$. Setting the probability P in Eq. 8 to p, the resulting fractile is given by:

$$u_{max,T,p} = \sqrt{2 \ln \left(\frac{N}{\ln\left(\frac{1}{p}\right)} \right)} \tag{9}$$

Consistent with Type I extreme value theory (e.g. [14] from [15]), the mean of $u_{max,T,p}$ is assumed to be well-approximated by its $p = 0.57$ fractile, so the expected value of the maximum of the Gaussian process

can be estimated by:

$$\mathrm{E}[U_{max}] = \sqrt{2\ln\left(\frac{N}{0.562}\right)} \tag{10}$$

It has been shown [16] that for problems such as those presented here, the result of Eq. 9, which is strictly based on the Poisson and Gumbel models, differs only slightly (e.g. 0.2%) from the classic Eq. 11 (e.g., [17]):

$$\mathrm{E}[U_{max}] \approx \sqrt{2\ln N} + \frac{0.577}{\sqrt{2\ln N}} \tag{11}$$

The expected value of the first-order maximum wave elevation is then:

$$\mathrm{E}[\eta_{1,max}] = \sigma_{\eta_1}\mathrm{E}[U_{max}] + m_{\eta_1} \tag{12}$$

The result of Eq. 10 or 11 is an estimate of the expected value of the maximum of a normal distribution which can be used directly in the Hermite model to predict non-Gaussian extreme values.

Non-Gaussian Extremes

The Hermite model assumes the non-Gaussian process $\eta(t)$ to be a cubic transformation of a standard Gaussian process $u(t)$. Hermite transformation, $g(u)$, can be conveniently written as a polynomial [18]:

$$\eta = g(u) = m_\eta + \kappa\sigma_{\eta_1}[u + c_3(u^2-1) + c_4(u^3-3u)] \tag{13}$$

For statistically "softening" processes, i.e. those with coefficient of kurtosis greater than 3 ($\alpha_4 > 3$), the variance of η is preserved by setting

$$\kappa = \left[1 + 2c_3^2 + 6c_4^2\right]^{-1/2} \tag{14}$$

in which the coefficients c_3 and c_4 control the shape of the distribution, i.e. preserve the desired skewness (α_3) and kurtosis (α_4). For processes that have relatively mild deviations from Gaussian behavior:

$$c_3 = \frac{\alpha_3}{4 + 2\sqrt{1 + 1.5(\alpha_4 - 3)}} \approx \frac{\alpha_3}{6} \tag{15}$$

$$c_4 \approx \frac{\alpha_4 - 3}{24} \tag{16}$$

Assuming the same transformation g in Eq. 13 applies at every point in time, including those points which are the maxima:

$$\mathrm{E}[\eta_{max}] = g(\mathrm{E}[U_{max}]) \tag{17}$$

in which $\mathrm{E}[U_{max}]$ can be conveniently estimated using Eq. 10.

Prediction of Extremes from First-order Diffraction Analysis

Two methods proposed by Sweetman and Winterstein [1] include non-linear, non-Gaussian effects as part of post-processing linear diffraction results. These methods are briefly discussed here for comparison with a

newly proposed method. In [1], the incident waves were considered a principal source of non-Gaussian effects; these effects were estimated by applying complete Stokes second-order transfer functions to the results of first-order diffraction analysis. The method is relatively rigorous from a physical standpoint: those terms being neglected from a complete second-order analysis are clearly identified. Unfortunately, the method is somewhat computationally intensive: it requires generation of a square matrix of second-order transfer functions which are combined with the transfer functions from first-order diffraction and the target seastate. An eigenvalue problem is then solved to determine the non-Gaussian statistical properties of the response.

A less computationally intensive approach based on narrow-band theory was also proposed in the same work [1]. This method assumes the maximum event as predicted from first-order theory coincides with that in second-order theory. Accordingly, a Stokes second-order correction is calculated at a single frequency and is applied to only the single maximum event predicted by first-order theory. The resulting method is computationally simple, but is an overly simplistic representation of the physical phenomenon. Also, use of the narrow-band assumption, which implies a worst-case phase locking, often over-predicts the observed maxima of the airgap demand.

A new method is proposed here in which a purely statistical correction based on the non-Gaussianity inherent to the incident waves is applied to the maximum airgap response process. The method is similar to that based on the Stokes second-order correction in that the incident waves are assumed to be a principle source of non-Gaussianity, but here the non-Gaussian effects are captured directly as statistical quantities, rather than physically through Stokes second-order transfer functions. The resulting method is computationally simple, yet does not rely on the narrow-band assumption.

Stokes Second-Order Correction

In this method post-processing first-order diffraction results, the only non-linear effects considered are those associated with the incident waves. This method is relatively rigorous from a physical standpoint in that the terms being neglected from a complete second-order analysis are clearly identified: in Eq. 4, all terms are included except $\eta_{2,d}$, which is assumed equal to zero. This method was previously proposed by Sweetman and Winterstein [1].

In modelling non-linear systems, it is common to employ Volterra series that enable estimation of a response quantity as a sum of first- and second-order transfer functions. For floating structures, these transfer functions are generally obtained from second-order hydrodynamic diffraction software packages such as WAMIT [3]. Here, Volterra series are used to calculate the free-surface elevation of the sea, η.

$$\eta(t) = \eta_1(t) + \eta_2(t) = \eta_1(t) + \eta_{2+}(t) + \eta_{2-}(t) \tag{18}$$

where $\eta_{2+}(t)$ and $\eta_{2-}(t)$ are the second-order sum and difference frequency contributions to the response.

Each of these quantities can be written in terms of first- and second-order transfer functions:

$$\eta_1(t) = \mathrm{Re}\sum_{k=1}^{n} A_k H_k^{(1)} e^{i\omega_k t} \tag{19}$$

$$\eta_{2+}(t) = \mathrm{Re}\sum_{k=1}^{n}\sum_{l=1}^{n} A_k A_l H_{kl}^{(2+)} e^{i(\omega_k+\omega_l)t} \tag{20}$$

$$\eta_{2-}(t) = \mathrm{Re}\sum_{k=1}^{n}\sum_{l=1}^{n} A_k A_l^* H_{kl}^{(2-)} e^{i(\omega_k-\omega_l)t} \tag{21}$$

in which $H_k^{(1)}$ denotes the first-order transfer function, and $H_{kl}^{(2+)}$ and $H_{kl}^{(2-)}$ are the second-order sum- and difference-frequency transfer functions and A_k and A_l are the complex Fourier coefficients of the incident wave process.

In a conventional second-order hydrodynamic analysis, $H_k^{(1)}$, $H_{kl}^{(2+)}$ and $H_{kl}^{(2-)}$ are all calculated by a diffraction program (e.g. WAMIT [3]). Here in Eq. 18, $\eta_1(t)$ is still to be separated into its incident and diffracted parts, $\eta_{1,i}(t)$ and $\eta_{1,d}(t)$, as in Eq. 4, with $H_k^{(1)}$ resulting from diffraction analysis. However, here $\eta_{2+}(t)$ and $\eta_{2-}(t)$ are calculated analytically from Stokes theory and $\eta_{2,d}$ is neglected.

The expected 3-hour maxima are ultimately predicted from the target seastate and these transfer functions using coefficients of skewness and kurtosis in a four-moment Hermite model. These statistical moments are calculated without realizing a time-history using methods originated by Kac & Seigert [19] and later expanded by Næss [20, 21]. The statistical moments are ultimately obtained by solving an eigenvalue problem. Problems such as these, which involve both sum and difference frequencies, lead to eigenvalue problems of size $2n$, twice the number of frequency components of $\eta_1(t)$. Implementation of the theory is described in [22], with extensions to airgap analysis from [6], and is further discussed in [1]. Results presented here use an optimization routine to minimize error in matching skewness and kurtosis values in the Hermite model (e.g., [22]).

Narrow-Band Model

In this method post-processing first-order diffraction results, the extreme of the total wave process, $\eta(t)$, is assumed to coincide in time with that of $\eta_1(t)$, so it is only necessary to model second-order effects during that single, largest wave cycle (Sweetman and Winterstein [1]). Performing load calculations for only the single most extreme event is the concept underlying the design wave approach. Longuet-Higgens [23] theoretically showed the peaks of a narrow-band Gaussian wave time-history follow a Rayleigh distribution. Other developments regarding application of narrow-band theory to ocean waves have been undertaken by Tayfun [24–27]. Applying a standard narrow-band model to the Gaussian process $\eta_1(t)$,

$$\eta_1(t) = a_\eta(t)\cos[\omega t + \theta_1(t)] \tag{22}$$

in terms of the slowly varying amplitude $a(t)$ and phase $\theta_1(t)$. (The instantaneous frequency ω may also be considered to be slowly varying.) The resulting second-order correction is:

$$\eta_2(t) = a_\eta^2(t) H^{(2+)}(\omega,\omega)\cos(2[\omega t + \theta_2(t)]) \tag{23}$$

in which $H^{(2+)}$ is the second-order sum frequency transfer function. The difference frequency transfer function, $H^{(2-)}$, for a sinusoidal input gives only a constant offset, which does not contribute to oscillations about the mean wave surface. Note that the narrow-band model effectively phase-locks the first- and second-order components, i.e $\theta_1(t) = \theta_2(t)$. In the largest wave cycle each process is assumed to attain a peak value at the same time (when both cosine terms are unity). At this time $a_\eta(t)$=$\eta_{1,max}$, so that the mean extreme of the total wave η=$\eta_1 + \eta_2$ is estimated as:

$$\mathrm{E}[\eta_{max}] = \mathrm{E}[\eta_{1,max}] + \mathrm{E}[\eta_{1,max}^2] H^{(2+)}(\omega,\omega) \tag{24}$$

The wave frequency, ω, should be "characteristic" of the seastate. The characteristic wave frequency, ω_c, is estimated here as $\omega_c = 2\pi/(0.92T_P)$, although results are expected to be relatively insensitive to this precise definition. Second-order Stokes theory in infinite water depth yields the expression $H^{(2+)} = k/2$. The wave number is defined by k=ω^2/g, in which g is the acceleration due to gravity. Thus, the maximum expected airgap demand can be estimated by:

$$\mathrm{E}[\eta_{max}] \approx \mathrm{E}[\eta_{1,max}] + \mathrm{E}[\eta_{1,max}^2]\frac{k}{2} \tag{25}$$

$E[\eta_{1,max}]$ is the that predicted by a conventional first-order hydrodynamic analysis with conventional first-order post-processing. The expected value of the square of $\eta_{1,max}$ is estimated by combining Eq. 10 with Type 1 extreme value theory (e.g., [17]) $\sigma^2_{\eta_1,max} = (\pi^2/6)(\sigma^2_{\eta_1}/(2\ln N))$ resulting in:

$$\begin{aligned} E[\eta_{1,max}^2] &= E[\eta_{1,max}]^2 + \sigma^2_{\eta_1,max} \\ &\approx \sigma^2_{\eta_1}\left[2\ln\left(\frac{N}{0.562}\right) + \frac{\pi^2}{6}\frac{1}{2\ln N}\right] \end{aligned} \tag{26}$$

Thus, the narrow-band approximation and Stokes second-order wave theory yield Eq. 25, which can be used to predict the total air-gap demand based on only $\eta_1(t)$ and its standard deviation, σ_{η_1}. These quantities can be readily predicted using only first-order theory.

Statistical Correction of First-Order Maxima

This new method of predicting a 3-hour maximum airgap demand based on results from first-order theory does not rely on a narrow-band approximation, but, again, approximates a second-order contribution using Stokes second-order theory. Here, the Hermite model, Eq. 13, is used with the coefficients of skewness and kurtosis based on just the incident waves to make a non-Gaussian estimate of the extreme value.

The first four moments of $\eta_i(t)$ are to be estimated using Stokes theory. Note that the coefficients of skewness and kurtosis, and therefore subsequent estimates of c_3, c_4 and κ are based on the incident wave only, and are merely assumed representative of the entire response process, including any diffraction effects. It is useful to associate T_p with a corresponding wave length of L_p, and steepness, S_p:

$$L_p = \frac{g}{2\pi} T_p^2 \tag{27}$$

$$S_p = H_s / L_p \tag{28}$$

The corresponding moments are then estimated as [28]:

$$\sigma_\eta = H_s/4 \tag{29}$$

$$\alpha_3 = 5.45\gamma^{-0.084} S_p \tag{30}$$

$$\alpha_4 = 3 + 1.41\alpha_3^2 \gamma^{0.02} \tag{31}$$

With these moments, the Hermite model is applied as Eqs. 13–14 to produce the non-Gaussian estimate of the mean maximum value.

Worked Example

The simplicity of application of the new method is demonstrated with a worked example. The mean-maximum non-Gaussian response is calculated for one location on the Veslefrikk semi-submersible for a sea-state with a significant wave height, H_s, of 14 m, peak period, T_p, of 13.5 s, and peakedness parameter, γ, of 3.

For this location, conventional post-processing of first-order diffraction yields an expected value of the maximum airgap demand, $\mathrm{E}[\eta_{1,max}]$, of 15.27 m and a standard deviation of that airgap demand, $\sigma_{\eta,1}$, of 3.924 m. Equations 27 and 28 are applied to find wave length and steepness representative of the sea spectrum.

$L_p = 284.26$ m

$S_p = 0.04925$

The coefficients of skewness and kurtosis, α_3 and α_4, of the response process (airgap demand) are estimated from Stokes theory using Equations 30 and 31.

$\alpha_3 = 0.2448$

$\alpha_4 = 3.0863$

The Hermite coefficients c_3 and c_4 and scaling factor κ are found from Equations 14 through 16.

$c_3 = 0.0408$

$c_4 = 0.003596$

$\kappa = 0.9983$

The Hermite polynomial can then be applied to transform the Gaussian estimate of the mean-maximum, $\mathrm{E}[\eta_{1,max}]$, to estimate the equivalent non-Gaussian extreme fractile, $\mathrm{E}[\eta_{max}]$. Here, the mean of the first-order prediction of the airgap demand, $m_{\eta,1}$, is equal to zero. The standard deviation of the first-order process, σ_u, equals $\sigma_{\eta,1}$. To predict the non-Gaussian mean-maximum, the standard-normal variable u is based on the mean-maximum of first-order prediction of the response, $\mathrm{E}[\eta_{max,1}]$, i.e. $u = (\mathrm{E}[\eta_{1,max}] - m_\eta)/\sigma_{\eta,1}$,

$\sigma_u = 3.924$ m

$u = 3.8914$

from which Equation 13 yields $\mathrm{E}[\eta_{max}] = \eta = 18.17$ m, which is the result shown on Figure 3. The first-order prediction of the mean-maximum is shown on the figure as "First-Order Only," and the final non-Gaussian result is shown as "First-Order with Statistical Correction".

Results

Results from each of the three methods discussed are also presented in Figure 3. The horizontal scales on the figures indicate airgap probe location as shown in Figure 2. All results are compared with measured data ("Measured"). Recall that all of these predictions are based on the same first-order diffraction analysis, and only the post-processing is being compared.

The solid line indicates the mean maximum of the measured data, which is calculated simply as the mean of the n maxima observed in each of the n realizations of each target seastate. As shown in Table 2, the number of seastates, n, is 5 for the 12 meter seastate and 6 for the 14 meter seastate. Error bars are calculated as the standard deviation of the n observations divided by $\sqrt{n}$.

The results denoted "First-Order Only" are those resulting from a first-order hydrodynamic analysis and conventional first-order post-processing. These first-order results under-predict nearly all of the measured data and all of the post-processing methods presented here.

The "Stokes Second-Order Correction" results can be observed to pass through roughly the middle of the measured data, but significantly under-predict at near-column locations (1, 4, 5, 6, and 9). Recall that this method includes the second-order effects in the incident waves, but not in the diffraction process or resulting diffracted waves. It is not surprising that this method under-predicts at those locations where diffraction effects are expected to be most extreme.

The remaining two sets of predictions, "Narrow-Band Model," and "Statistical Correction of First-Order Maxima" show greater predicted maxima than the other methods. There is close agreement between these

two predictions because both methods account for the same physical effects: second-order effects in both the incident waves and the diffracted waves are included in both methods, and in both methods those second-order effects are estimated from Stokes second-order theory. Also, both methods neglect any second-order diffraction effects.

The differences between these methods lie in how these effects are considered. The narrow band model implicitly assumes that second-order effects are captured as the *one* second-order wave which would be associated with the largest predicted first-order wave. This one wave has amplitude based on Stokes theory, and has period characteristic of the entire sea-state. The narrow-band assumption effectively phase-locks these first- and second-order wave components so the first-and second-order components are additive. This phase-locking is not inconsistent with Stokes theory. Note that it is implicitly assumed that the diffracted waves behave as do incident waves, i.e. in accordance with Stokes theory.

The method based on statistical correction employs estimates of the coefficients of skewness and kurtosis for the entire sea-state, and uses these statistical moments to transform the first-order Gaussian predicted maximum to a nonlinear non-Gaussian prediction. As in the narrow-banded model, it is implicitly assumed that the diffracted waves behave as do incident waves, i.e. in accordance with Stokes theory. However, there is no assumption that all second-order components act together as one equivalent wave, nor is there an assumption of narrow banded behavior (phase locking).

These two prediction methods roughly agree in magnitude, which is not surprising because they each attempt to capture, and to neglect, the same physical effects. For practical use, the method based on the statistical correction is preferred because it hinges on fewer underlying assumptions and because it is quite straightforward to apply.

All of the methods presented here which include some second-order effects yield results better match measured data than results from first-order theory alone. Unfortunately, none of the methods show adequate spatial variation. This inadequacy results from the fact that in all three methods, the second-order effects are all predicted from Stokes wave theory, which does not include any spatial variation.

Airgap Prediction based on Model Test Data

The preceding sections have considered various methods of predicting expected maxima based on diffraction results. While each of these methods enables better prediction results than conventional post-processing of first-order diffraction results, none of them offers the spatial variability observed in physical model tests. It has also been previously shown [7, 30] that in some cases, industry standard second-order diffraction analysis produces unrealistically large amplitude response due to excessive second-order transfer functions at high frequencies. Without improvements to second-order diffraction analysis, inclusion of model testing as part of final design seems prudent. This section considers prediction of airgap demand maxima based on model

test results for use in final design.

In [2], Winterstein and Sweetman inferred linear regression parameters directly from measured model test data; these parameters could then be used to predict fractiles of airgap demand. The focus of that work was relating fractiles of the incident and diffracted waves and development of amplification factors from diffraction analysis for prediction of airgap extremes.

Here, a new method is proposed which is an application of the fractile-based method from [2]. Instead of relating fractiles of the incident waves to those of the diffracted waves as in [2], here incident wave fractiles are predicted directly from statistical theory, and then used in conjunction with amplification factors derived from model test data to predict extreme values of the diffracted waves. The first- and second-order extreme value theories applied are those discussed earlier in this paper. The regression theory is that resulting from [2]. The purpose of this method is to extract robust estimates of extreme values from model test data.

The extreme value of the first-order incident wave, $\eta_{1,max}$, is determined from statistical theory using Eq. 10 and Eq. 12. The number of waves, N in Eq. 10, can be grossly estimated as the test duration divided by the peak period, T_p, or more accurately as the test duration divided by the mean up-crossing period, T_z, which can be approximated by [29]:

$$T_z = \frac{T_p}{1.49 - 0.102\gamma + 0.0142\gamma^2 - 0.00079\gamma^3} \tag{32}$$

where γ is the peakedness parameter associated with the JONSWAP sea spectrum (e.g. [9] from [10]).

The value of $\eta_{1,max}$ resulting from Eq. 12 is then transformed to include Stokes second-order effects on the non-Gaussian third and forth statistical moments through use of the Hermite transformation (Eqs. 13–17), in which the third and fourth statistical moments α_3 and α_4, can be estimated using Eqs. 30 and 31.

The regression parameter b_p resulting from measured data is combined with the resulting estimate of $\eta_{i,max}$ to predict η_{max}. Two parameters result from the development in [2]:

$$b_p = \sigma_Y/\sigma_X\,; \quad \text{and}\,; \quad a_p = m_Y - b_p m_X \tag{33}$$

The means and standard deviations, m and σ, in Eq. 33 are those of the peaks alone, i.e. the the maxima between zero up-crossings, and not of the entire process. The regression parameter a_p is the y-intercept of a linear regression, or, physically, the peak height of the response, Y_p, expected to result from an incident wave peak of height X_p. For these problems, $a_p = 0$, or $Y_p = b_p X_p$. The expected maximum of the wave surface elevation, $\mathrm{E}[\eta_{max}]$, can be estimated as:

$$\mathrm{E}[\eta_{max}] = b_p \mathrm{E}[\eta_{i,max}] = \frac{\sigma_Y}{\sigma_X}\mathrm{E}[\eta_{i,max}] \tag{34}$$

This methodology enables a robust prediction of the expected maxima from limited model test data; for example, if only two realizations of the sea-state were performed, this method could be employed to provide two additional estimates of the mean maximum (one from each test), or one more robust estimate (con-

catenating all test data). Application of this method would be prudent for any model test, but would seem particularly attractive if there is a substantial difference between the maxima observed in various tests.

Another useful application is prediction of maxima for a sea-state having the same peak period, T_p, and steepness parameter, γ, as the target sea-state realized in a model test, but a different significant wave height, H_s. First-order hydrodynamic theory suggests that b_p is a function of the vessel and the shape of the sea-spectrum, but not of the significant wave height. Note that in any application, the transformation from the incident wave to the airgap response must behave as a stationary process for the predicted maxima to be meaningful.

In the following section, maxima predicted using Eq. 34 are compared with the actual means of measured data.

Results from Predictions based on Model Test Data

Figure 4 demonstrates the utility of Eq. 34. The figure shows, somewhat paradoxically, that the single maximum value observed in a model test is not necessarily a good estimate of the maximum value that should be observed in that model test, i.e. the test itself may result in a statistically unlikely maximum value. The line denoted "Measured" is the same measured data as presented on other figures. These measured maxima are calculated by averaging the maximum observed in each of the n model tests and are considered a best estimate of each of the mean maxima. The line denoted "Worst Realization" represents the maxima observed at each of the nine airgap probe locations during the single test whose maxima most poorly agreed with the average of the observed maxima, i.e. results from that test having the most outlying data points. The line entitled "Regression: $b_p\eta_{i,max}$" represents the maxima predicted using Eq. 34 and b_p calculated from data measured *only* in the seastate denoted "Worst Realization."

Figure 4 compellingly demonstrates that the statistical prediction of the expected maximum is a far more reliable predictor of the expected maximum than is the *one* maximum actually observed in the model test basin. The practical implication is that it would be prudent to do a statistical analysis of model test data to provide a more robust prediction of the extreme values expected for design purposes. The statistical analysis would be particularly prudent when only limited test data are available.

Conclusions

Two new methods of predicting airgap demand have been presented. The first new method enables inclusion of some second-order effects, though it is based on only first-order diffraction results. The new method and two existing methods have been compared with each other and with model test data. All three methods yield results superior to those based on conventional post-processing of first-order diffraction results, and

comparable to optimal post-processing of second-order diffraction results. The newly proposed method is recommended for use in the early stages of design because it simple enough to be implemented as a hand calculation yet yields results far superior to conventional post-processing of first-order diffraction results. None of the methods presented here is adequate for use in final design; it is believed that use of model testing is appropriate for final design.

The second new method to be presented is appropriate for use in final design. It combines extreme value theory with statistical regression to predict extreme airgap events using model test data. Estimates of extreme airgap events based on this method are found to be more reliable than estimates based on only extreme observations from a single model test. This second new method is suitable for use in the final stages of design.

Prediction of extremes from first-order diffraction

The first of the two new methods is based on a statistical correction to first-order diffraction results. The underlying assumptions inherent to the new method are straightforward. The method is also simple to apply and yields results comparable to post-processing methods which are much more difficult to apply or which rely on more assumptions. Two existing methods have also been briefly presented and discussed for explanation of the theoretical background and for comparison of results with the new method. Each of the three methods applies some second-order correction based on Stokes second-order wave theory. One of the methods, perhaps the most theoretically rigorous of the three, requires solution of an eigenvalue problem. The next two methods, one based on narrow-band theory and the other based on a statistical correction, are each numerically simple enough to be performed by a simple computer algorithm or as hand calculations.

Figure 3 compares the results of these three methods with measured data and with results from a conventional first-order analysis. The "First-Order with Statistical Correction" was observed to predict airgap demand values between those of the "Narrow Band Model" and the "Stokes Second-Order." All of these methods yield results that better agree with observed data than do those resulting from conventional first-order post-processing.

Figure 5 compares results from the "First-Order with Statistical Correction" with those of "First-Order Only", " 'Best' Second-Order" and with "Measured" data. The predictions based on linear diffraction plus a statistical correction agree with measured data about as well as those based on optimized post-processing of second-order diffraction results. These " 'Best' Second-Order" results are based on results of a full second-order analysis, with the high frequency second-order transfer function terms from the diffraction analysis replaced by those from Stokes theory [7, 30]. These "Best" results are believed to be the the most accurate prediction that can be generated using second-order diffraction. It has been shown through use of system identification that the high-frequency second-order transfer functions were dramatically over-predicted by this second-order diffraction analysis [7, 16], and that inclusion of these spurious quadratic transfer functions

results in dramatic over-prediction of the airgap demand; the resulting excessive predictions are not believed to be meaningful and are not shown or considered here. Also note that the observed variability between the first-order results in Figure 3 and Figure 5 is because they result from WAMIT analyses using a different frequency grid and slightly different surface meshing.

Considering all of the results presented in Figures 3 and 5, any of the methods of including second-order effects with results from first-order diffraction increases the prediction of the mean maximum from the "First-Order Only" result to more nearly approximate that of observed model test data. The magnitude of the predicted peak is generally centered amongst the measured data (Stokes), or slightly above most of the data (Narrow Band and Statistical Correction). However, all of these predictions fail to adequately follow the trend in observed extremes at near-column locations.

Inclusion of second-order effects in airgap predictions is important at every stage of design. Second-order effects often make the airgap demand more severe, and sometimes substantially so. The new method presented here is simple to apply and captures significant second-order effects. Applying this new method in the early stages of design would improve the early design and would reduce the likelihood of airgap surprises later in the design process. The "Stokes second-order correction" is theoretically more rigorous, but makes no attempt to capture non-linear effects in the diffracted wave. In later stages of design it may be appropriate to use this "Stokes" correction in addition to some other methodology intended to capture second-order effects in the diffracted waves.

While all of these methods provide results superior to conventional post-processing of first-order diffraction results, they fail to predict sufficient spatial variability to be considered a realistic alternative to model testing for final design. A robust second-order diffraction analysis would seem to provide the best hope to capture these highly non-linear effects. Unfortunately, second-order diffraction [31] has also been shown ineffective for certain kinds of airgap problems [1]. Until better second-order diffraction methods are developed, final design will continue to rely on physical model testing.

Prediction of extremes from model test results

Another new method has also been presented which is used to predict extreme values of airgap demand from model test data. Statistical theory and regression of measured data are applied to predict these extreme values.

The method has been demonstrated (Figure 4) to provide an estimate of the maximum that is more reliable than is an estimate based on the maximum observed in a single model test. The method should be used to predict expected maxima for design purposes and can be used to apply model test results to sea-states with significant wave heights different than those physically tested. Application of this method is appropriate for interpretation of model test results in preparation for final design.

Acknowledgements

Parts of this work resulted from the doctoral and post-doctoral work of the author at Stanford University. The author wishes to gratefully acknowledge the guidance and support of his Post-Doctoral advisor, Professor C. Allin Cornell and his PhD co-advisors Doctor Steven R. Winterstein and Professor C. Allin Cornell. The author would also like to thank all the RMS project sponsors and especially Statoil, for making available the wave tank data and the WAMIT hydrodynamic analysis of the Veslefrikk platform.

Nomenclature

α_3 Third statistical moment, skewness.

α_4 Fourth statistical moment, coefficient of kurtosis.

δ Vertical motion of the platform with frame of reference fixed to the platform.

η Local wave elevation, including both incident wave and diffraction effects

η_1 First-order part of η

$\eta_{1,i}$ First-order part of η_i

$\eta_{1,max}$ Maximum value of first-order part of η

$\eta_{1,d}$ First-order part of η_d

η_2 Second order part of η

η_{2+} Sum-frequency contribution to second-order wave response

η_{2-} Difference-frequency contribution to second-order wave response

$\eta_{2,d}$ Second-order part of η_d

$\eta_{2,i}$ Second-order part of η_i

η_d Additional wave elevation caused by diffraction effects

η_i Incident wave elevation

$\eta_{i,max}$ Maximum incident wave

η_{max} The maximum value of η, e.g. the largest observed sea-surface elevation in a three-hour period.

γ Spectral peakedness parameter, as for JONSWAP spectrum

κ Scaling coefficient used in the Hermite polynomial

ν_o average up-crossing rate of a random process

ω Instantaneous frequency of wave process

ω_c Wave frequency characteristic of a sea-state

ω_k, ω_l Fourier frequencies of wave process

σ_η Standard deviation of the wave elevation

$\sigma_{\eta,1}$ Standard deviation of η_1

$\sigma_{\eta_1,max}$ Standard deviation of $\eta_{1,max}$

σ_X Standard deviation of incident wave peaks

σ_Y Standard deviation of wave peaks in the presence of the model

θ_1 Phase shift of η_1 in narrow-band model

θ_2 Phase shift of η_2 in narrow-band model

ξ_3 Vessel heave

ξ_4 Vessel roll

ξ_5 Vessel pitch

A_k, A_l Complex Fourier coefficients of incident wave process

A_l^* Complex conjugate of A_l

a Airgap at a specific location on the platform; the vertical distance between the sea surface and lowest part of the platform deck

$a_\eta(t)$ Slowly varying amplitude of η_1

a_0 Still-water airgap

a_p Regression parameter for model test data (intercept)

b_p Regression parameter for model test data (slope)

c_3, c_4 Coefficients used in the Hermite polynomial

f Circular frequency, $1/t$

g Acceleration due to gravity

$H_k^{(1)}$ First-order transfer function from hydrodynamic diffraction.

$H_{kl}^{(2+)}$ Sum-frequency second-order transfer function from hydrodynamic diffraction.

$H_{kl}^{(2-)}$ Difference-frequency second-order transfer function from hydrodynamic diffraction.

H_s Significant wave height

k Wave number, ω^2/g.

L_p Wave length associates with T_p

m_η Mean of the wave process

m_{η_1} Mean of the first-order wave process

m_X mean of the peaks of an incident wave process

m_Y mean of the peaks of the wave process in the presence of the model

N Number of cycles in a random process

n number of realizations of a single sea-state

p Probability of an event

S_p Wave steepness associated with T_p, H_s/L_p

$S_\eta(f)$ Spectral density function of the sea-state

T Duration of a random process.

T_P Spectral peak period

T_{SS} Duration of a sea-state for which the random process model is assumed fixed

T_z Mean up-crossing period

t Time

U A reference standard-normal random variable

U_{max} The maximum value of U

u A reference value in standard-normal random process

$u_{max,T,p}$ The expectation for the maximum value of u for specified T and p.

$u(t)$ A reference standard-normal random process

X Height of an incident wave peak

X_p Height X occurring with probability p

Y Height of a wave peak in the presence of the model

Y_p Height Y occurring with probability p

x Location with frame of reference fixed to the platform

y Location with frame of reference fixed to the platform

References

[1] Sweetman, B. and Winterstein, S. R., 2003. Non-Gaussian Air Gap Response Models for Floating Structures. ASCE Journal of Engineering Mechanics, 129, 3, pp. 302–309.

[2] Winterstein, S. R. and Sweetman, B., 2001. Air Gap Response of Floating Structures: Statistical Predictions vs Observed Behavior. ASME Journal of Offshore Mechanics and Arctic Engineering, 123, pp. 118–123.

[3] WAMIT 5.3, 1999. *WAMIT: User Manual Versions 5.4, 5.4PC, 5.3S.* Dept. of Ocean Engineering, M.I.T.

[4] Teigen, P. and Trulsen, K., 2001. Numerical Investigation of Non-linear Wave Effects around Multiple Cylinders. In *Proc., Intl. Offshore Polar Eng.* ISOPE.

[5] Manuel, L., Sweetman, B., and Winterstein, S. R., 2001. Analytical Predictions of the Air Gap Response of Floating Structures. Journal of Offshore Mechanics and Arctic Engineering, 123, pp. 112–117.

[6] Manuel, L. and Winterstein, S. R., 2000. Reliability Based Predictions of a Design Air Gap for Floating Offshore Structures. In *Proceedings 8'th ASCE Conf. on Probablistic Mechanics and Structural Reliability.* ASCE.

[7] Sweetman, B., Winterstein, S. R., Meling, T. S., and Birknes, J., 2001. Airgap Prediction: Use of Second-Order Diffraction and Multicolumn Models. In *Proceedings, ISOPE 2001-IL-13, available from www.rms-group.org.* International Society of Offshore and Polar Engineers.

[8] Fokk, T., 1995. Veslefrikk B Air Gap Model Tests. Tech. Rep. 512167.00.01, MARINTEK Trondheim, Norway.

[9] Sarpkaya, T. and Issacson, M., 1981. *Mechanics of Wave Forces on Offshore Structures.* Van Nostrand Reinhold Company.

[10] Hasselmann, K., Barnett, T. P., Bouws, E., H. Carlson, H., Cartwright, D. E., Enke, K., Ewing, J. A., Gienapp, H., Hasselmann, D. E., Kruseman, P., Meerburg, A., Mller, P., Olbers, D. J., Richter, K., Sell, W., and Walden, H., 1973. Measurements of Wind-Wave Growth and Swell Decay during the Joint North Sea Wave Project (JONSWAP). Deutschen Hydrographischen Zeitschrift, 12.

[11] Clough, R. W. and Penzien, J., 1975. *Dynamics of Structures.* McGraw-Hill.

[12] Cartwright, D. and Longuet-Higgins, M. S., 1956. The Statistical Distribution of the Maxima of a Random Function. Proceedings of the Royal Society of London, A237, pp. 212–232.

[13] Davenport, A., 1964. Note on the Distribution of the Largest Value of a Random Function with Application to Gust Loading. Proceedings of the Institution of Civil Engineers, 28, pp. 187–196.

[14] Benjamin, J. R. and Cornell, C. A., 1970. *Probability, Statistics and Decision for Civil Engineers.* McGraw-Hill.

[15] Gumbel, E. J., 1958. *Statistics of Extremes.* Columbia University Press, New York.

[16] Sweetman, B., 2001. Airgap Analysis of Floating Structures subject to Random Seas: Prediction of Extremes using Diffraction Analysis versus Model Test Results. Ph.D. thesis, Stanford University.

[17] Madsen, H. O., Krenk, S., and Lind, N. C., 1986. *Methods of Structural Safety.* Prentice-Hall, Inc., New Jersey.

[18] Winterstein, S., 1988. Nonlinear vibration models for extremes and fatigue. Journal of Engineering Mechanics ASCE, 114, pp. 1772–1790.

[19] Kac, M. and Siegert, A. J. F., 1947. On the theory of noise in radio receivers with square law detectors. Journal of Applied Physics, pp. 383–400.

[20] Næss, A., 1986. The Statistical Distribution of Second-Order Slowly-Varying Forces and Motions. Applied Ocean Research, 8, pp. 110–118.

[21] Næss, A., 1992. Prediction of extremes related to the second-order, sum-frequency response of a TLP. In *Proc., 2nd Intl. Offshore Polar Eng.* ISOPE.

[22] Winterstein, S. R., Ude, T. C., and Marthinsen, T., 1994. Volterra Models of Ocean Structures: Extreme and Fatigue Reliability. Journal of Engineering Mechanics, 120, pp. 1369–1385.

[23] Longuet-Higgins, M. S., 1952. On the Statistical Distribution of the Heights of Sea Waves. Journal of Marine Research, 11, pp. 245–266.

[24] Tayfun, M. A., 1980. Narrow-Band Nonlinear Sea Waves. Journal of Geophysical Research, 85, pp. 1548–1552.

[25] Tayfun, M. A., 1986. On narrow-band representation of ocean waves: 1. Theory. Journal of Geophysical Research, 91, pp. 7743–7752.

[26] Tayfun, M. A., 1986. On narrow-band representation of ocean waves: 2. Simulations. Journal of Geophysical Research, 91, pp. 7753–7759.

[27] Tayfun, M. A. and Lo, J.-M., 1989. Envelope, phase and narrow-band models of sea waves. Journal of Waterway, Port, Coastal, and Ocean Engineering, 115, pp. 594–613.

[28] Jha, A. K. and Winterstein, S. R., 2000. Nonlinear Random Ocean Waves: Prediction and Comparison with Data. In *Proceedings of the 19th International Conference on Offshore Mechanics and Arctic Engineering*.

[29] Chakrabarti, S. K., 1987. *Hydrodynamics of Offshore Structures*. Springer-Verlag.

[30] Sweetman, B., Winterstein, S. R., and Cornell, C. A., 2002. Air Gap Response of Floating Structures: First and Second-Order Transfer Functions from System Identification. Journal of Applied Ocean Research, 24, 2, pp. 107–118.

[31] WAMIT 4.0, 1995. *WAMIT: A Radiation-Diffraction Panel Program for Wave-Body Interactions–User's Manual*. Dept. of Ocean Engineering, M.I.T.

Platform Particulars	
Length Over All (LOA):	107.50 m
Longitudinal Column Spacing:	68.00 m
Transverse Column Spacing:	67.00 m
Column Length w/o Sponson:	12.50 m
Column Breadth:	12.50 m
Pontoon Breadth:	14.25 m
Pontoon Height:	9.50 m
Test Conditions	
Draft, D:	23.00 m
Displacement:	40,692 tonnes
Airgap to Still Water Level:	17.50 m
Center of Gravity (from keel):	24.13 m
Pitch Radius of Gyration:	33.76 m
Roll Radius of Gyration:	34.26 m
Transverse Metacentric Height:	2.36 m
Water Depth:	175.00 m

Table 1: Characteristics of Veslefrikk platform.

H_S [m]	T_P [s]	γ	Number of 3-hour tests	Spectral Type
12.0	11.5	4.0	5	Bimodal
14.0	13.5	3.0	6	JONSWAP

Table 2: Seastate parameters for which model tests data is analyzed.

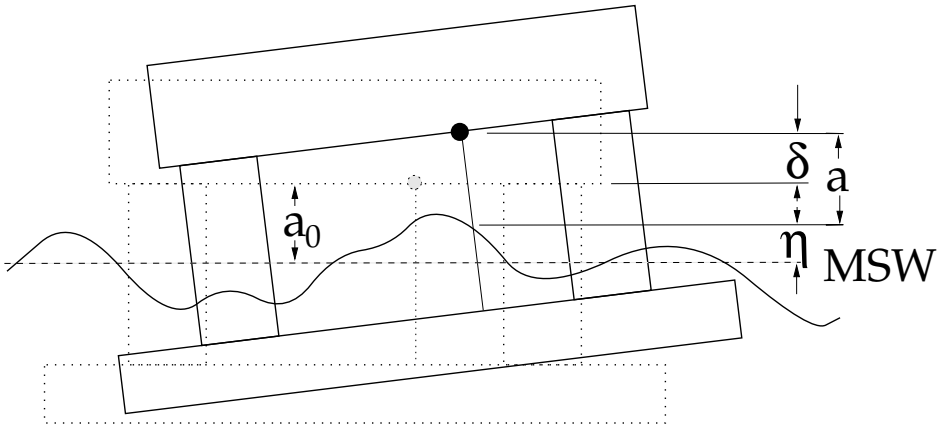

Figure 1: Airgap Variable Definitions

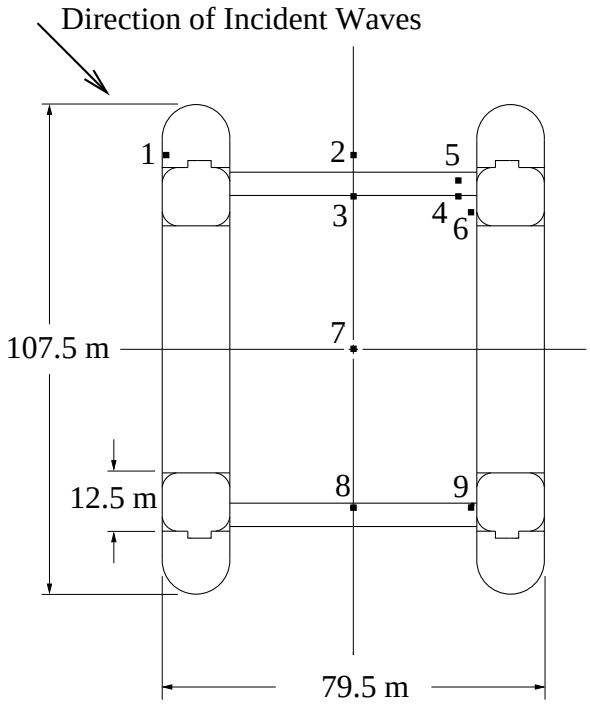

Figure 2: Plan view of Veslefrikk platform and location of airgap probes.

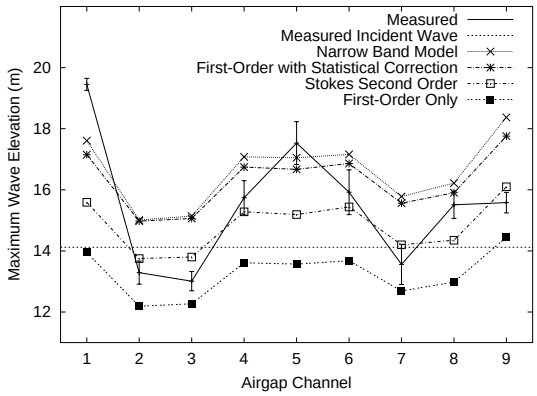

$H_s = 12$ m, $T_p = 11.5$ sec.

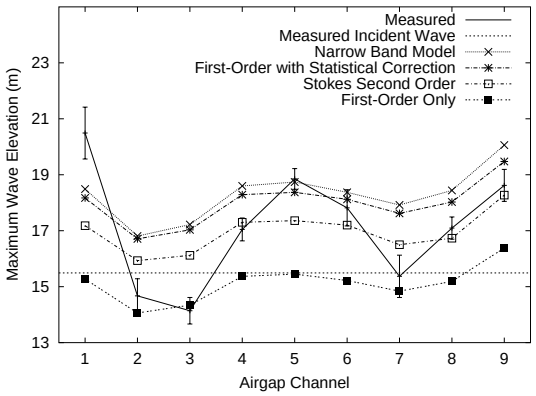

$H_s = 14$ m, $T_p = 13.5$ sec.

Figure 3: Measurement data compared with predictions of maximum airgap demand based on various corrections to first-order analysis

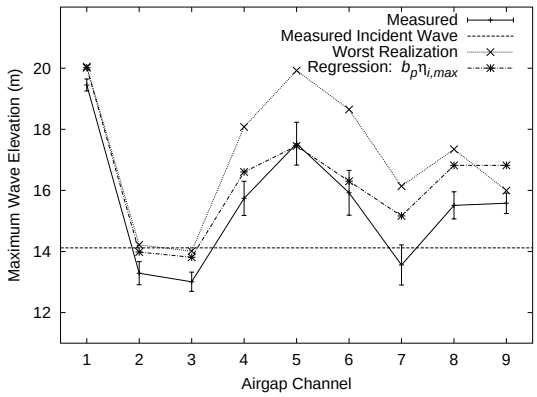

$H_s = 12$ m, $T_p = 11.5$ sec.

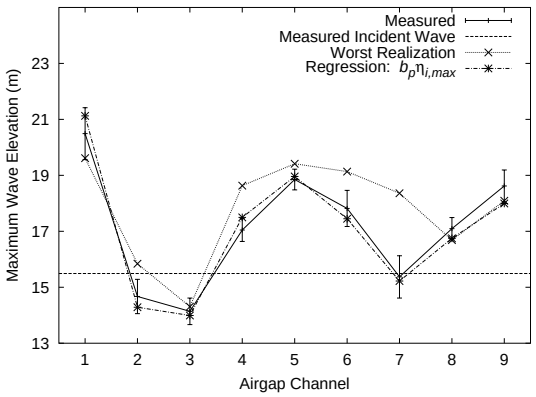

$H_s = 14$ m, $T_p = 13.5$ sec.

Figure 4: Average and worst-behaved observed maxima compared with predictions resulting from Eq. 34 and that worst-behaved seastate.

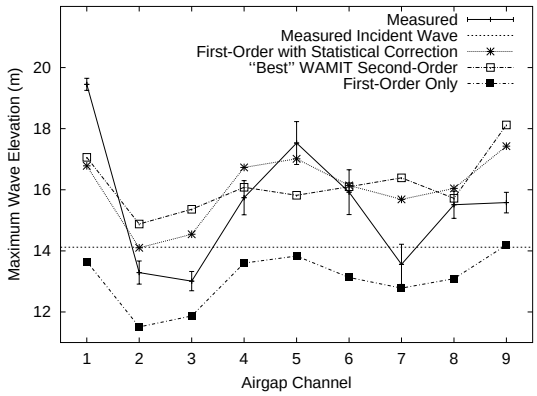

$H_s = 12$ meters, $T_p = 11.5$ seconds

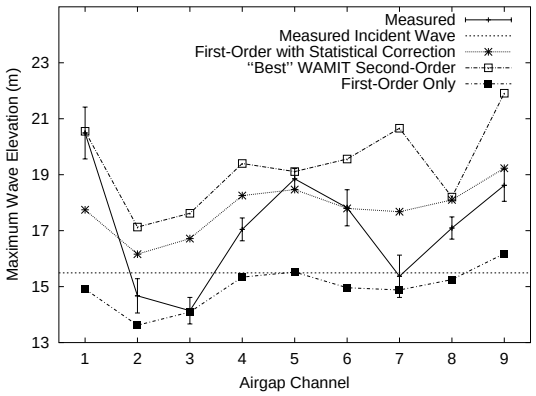

$H_s = 14$ meters, $T_p = 13.5$ seconds

Figure 5: Measurement data compared with predictions of maximum airgap demand based on first-order analysis, full second-order theory, and first order with a statistical correction